IEEE Access
Multidisciplinary | Rapid Review | Open Access Journal

Received June 16, 2020, accepted June 27, 2020, date of publication July 1, 2020, date of current version July 16, 2020.

Digital Object Identifier 10.1109/ACCESS.2020.3006239

Long-Term Frequency Stability Assessment Based on Extended Frequency Response Model

YUZHENG XIE[1], CHANGGANG LI[1], (Member, IEEE), HENGXU ZHANG[1], (Member, IEEE), HUADONG SUN[2], (Senior Member, IEEE), AND VLADIMIR TERZIJA[3]

[1]Key Laboratory of Power System Intelligent Dispatch and Control of the Ministry of Education, Shandong University, Jinan 250061, China
[2]China Electric Power Research Institute, Beijing 100192, China
[3]School of Electrical and Electronic Engineering, University of Manchester, Manchester M60 1QD, U.K.

Corresponding author: Changgang Li (lichgang@sdu.edu.cn)

This work was supported in part by the State Key Laboratory of HVDC, Electric Power Research Institute, China Southern Power Grid, under Grant SKLHVDC-2019-KF-15, and in part by the Young Scholars Program of Shandong University under Grant 2018WLJH31.

ABSTRACT Large frequency deviation degrades the operation performance of the boiler and its auxiliaries. It affects the output of thermal power units. A significant change in power generation leads to a great frequency deviation. An extended frequency response model for long-term frequency stability assessment is constructed to consider the effects of frequency deviations on boiler auxiliaries. The static power-frequency characteristic of the thermal power unit within an extensive frequency variation range is analyzed. It reveals that the active power output of the generating unit is not monotonically increasing with frequency dropping. An inflection point is observed on the static power-frequency characteristic curve when considering boiler auxiliary frequency characteristics. In the range of greater frequency deviation, the output power decreases rapidly with frequency declination, and an unstable equilibrium point (UEP) of frequency stability is identified. A quantitative index is proposed for frequency stability assessment based on UEP. The stability characteristic and the frequency stability quantitative index based on UEP are analyzed. The frequency dynamic behaviors of the extended model are demonstrated to analyze frequency stability characteristics within an extensive frequency variation range by a single machine system and the IEEE 39-bus system with considering boilers and its auxiliaries.

INDEX TERMS Power system, thermal power plant, auxiliaries, frequency stability.

I. INTRODUCTION

Frequency is one of the most significant variables indicating the security and stability of the power system. High penetration of renewable energy sources decreases power system inertia [1]. It results in a large frequency deviation for some disturbances with great power deficit [2], [3]. Large frequency deviation affects system active power control. It even leads to blackouts, such as the cases in South Australia [4] and London [5]. Power system frequency security and stability controls are facing new challenges [6], [7]. Therefore, it is necessary to study power system frequency dynamic behavior and stability within an extensive frequency deviation range.

Frequency stability is the ability of a power system to maintain steady frequency following a significant imbalance between generation and load [8]. With the development of renewable energy, frequency dynamic behaviors are more complex and intense, which even lead to frequency instability in extreme situations [9]–[11]. So far, frequency stability studies mostly focus on frequency dynamic response analysis, under frequency load shedding (UFLS) scheme configuration [12], and quantitative evaluation of frequency control techniques [13], [14]. Due to the rare occurrence of frequency instability cases, most of those studies are mainly based on frequency response simulation with the methods of three categories: full-time domain numerical simulation model [15], average system frequency model (ASF) [16], and system frequency response model (SFR) [17], [18]. Most of the power systems are mainly composed of the thermal power unit. The controllability of the thermal power unit output power is better than the other types of generating units. The frequency response simulation models mainly consider the frequency characteristics of thermal power units. The full-time domain simulation is a commonly used method to

The associate editor coordinating the review of this manuscript and approving it for publication was Lin Zhang.

obtain system frequency response. It has been implemented in electromechanical transient simulation programs, such as PSS/E and DSA Tools. ASF model aggregates the rotor swing equations of all generators and ignores the effect of the voltage and the network. It roughly reflects system frequency dynamic behaviors. If the turbine-governors are aggregated into a single model, the ASF model becomes a single machine model. If the nonlinear parts of the single machine model are simplified, the SFR model is derived to analytically solve the maximum frequency deviation and the corresponding time with a given disturbance [18]. These methods usually assume the boiler steam pressure is constant or infinite within a small frequency deviation range. They are only suitable for short-term frequency dynamic study. However, due to the devices with slow dynamics, they cannot be used in the scenario with large frequency deviations. Boiler and its auxiliaries are ignored to speed up a simulation with the assumption of infinite boiler stored energy [19].

However, the boiler cannot be overlooked when considering the long-term frequency dynamics following severe upsets. In the long-term studies, the stored energy in the boiler is limited in actual operation. It affects the primary frequency regulation of the generator and the maximum frequency deviation [20], [21]. Reference [22] considered the dynamic behaviors of the boiler to reflect system frequency dynamic behaviors following disturbances. Reference [23] indicated that the control valve opening following a severe disturbance results in a quick reduction of boiler steam pressure. Reference [24] proposed that boiler steam pressure is related to feedwater and fuel regulation. Feedwater pumps and coal mills are driven by induction motors. The induction motor speed varies with frequency decreasing, which degrades the performance of auxiliaries. Large frequency deviations make the output of auxiliaries in power plant reduce dramatically and affect boiler steam pressure. Boiler operation condition change affects the mechanical power of the steam turbine, and then it affects frequency dynamic behaviors. Therefore, it is necessary to consider the power-frequency characteristics of the auxiliaries in long-term frequency characteristics analysis. Reference [25] constructs a simplified closed-loop control model, including a boiler, pulverizing system, and auxiliary regulation system. However, the power-frequency characteristic of the auxiliaries was not considered.

The conventional frequency response model does not consider the frequency characteristic of the auxiliaries and ignores the effects of frequency deviations on the output of the boiler and its auxiliaries. In this premise, the output power of the thermal power unit increases monotonously with the frequency dropping. It is only suitable for the scene with the frequency varying near the rated value. However, if the frequency drops greatly, the output of the boiler and auxiliaries are affected and reduced. It changes the output power and the static power-frequency characteristic curve of the thermal power unit within a large frequency deviation range. Therefore, frequency dynamics and stability analysis should be extended to an extensive frequency variation range.

In this paper, 1) an extended single machine frequency response model is constructed to analyze the static power-frequency characteristic to the thermal power unit and long-term frequency stability within an extensive frequency variation range. The extended model considers the effects of frequency deviations on the output of boiler auxiliaries. 2) The static power-frequency characteristic of the thermal power unit within an extensive frequency variation range is obtained and analyzed with the extended model. It reveals that the output power of the generating unit is no longer monotonically increasing with frequency dropping. There is an inflection point on the static power-frequency characteristic curve of the generator. 3) The static power-frequency characteristic curves of the generating unit and load have two equilibrium points. Both of the equilibrium points can satisfy the balance between generation and load. According to their static stability characteristic, one of the equilibrium points with a large frequency deviation is defined as the frequency unstable equilibrium point (UEP). A quantitative index is proposed for frequency static stability assessment based on UEP.

The rest of this paper is organized as follows. In section II, the physical structure of the thermal power unit is illustrated. An extended single machine frequency response model is constructed, considering the effects of frequency deviations on boiler auxiliaries. In section III, the static power-frequency characteristic of the thermal power unit is obtained and analyzed within an extensive frequency variation range. The definition and stability characteristics of UEP are elaborated. In section IV, a quantitative index for frequency static stability assessment is proposed to assess the frequency stability degree under different load characteristics based on UEP. The single machine system and IEEE 39-bus system are used to verify the validity in section V. Conclusions are drawn in Section VI.

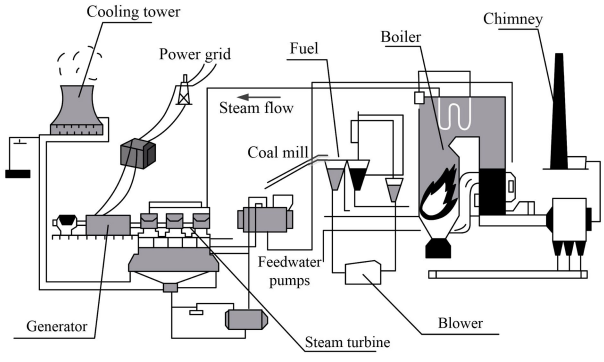

FIGURE 1. The physical diagram of the thermal power unit.

II. THE EXTENDED FREQUENCY RESPONSE MODEL

A. THE PHYSICAL STRUCTURE OF THE THERMAL POWER UNIT

The physical structure of the thermal power unit is shown in Fig.1. The boiler system provides steam flow to the

steam turbine. Steam turbine transfers steam flow to mechanical power. In the generator, the mechanical power is converted into the electromagnetic power transmitted to the power grid. The power grid frequency is the feedback signal to regulate auxiliary operation. Boiler combustion is determined by feedwater flow, fuel flow, and airflow supplied by the auxiliaries, such as feedwater pump, coal mill, and blower. According to the thermal power plant investigation, these auxiliaries are driven by induction motors. The traditional induction motors are sensitive to frequency change. However, the variable-frequency motors are not. Large transient frequency reduction decreases the speed severely of the conventional induction motor. It results in motor stalling in extreme conditions, which leads to the boiler, and the generator stopped working. This paper mainly considers the auxiliaries equipped with the traditional induction motor.

In the boiler system, the evaporation process is completed in the boiler. The heating surface boundary of the boiler varies with the ratio between feedwater flow and fuel flow change. Fuel or feedwater change affects the boiler operating conditions. The boiler working condition is regulated to maintain the ratio between feedwater and fuel within the desired range. It makes boiler feedwater flow, and fuel flow satisfies boiler evaporation requirements, which further regulate the steam flow of steam turbines to meet load change. The feedwater flow is consistent with the steam flow and approximately proportional to the load.

In the thermal power unit, the auxiliaries, the boiler combustion, the steam turbine, and the generator form a closed-loop feedback system. When frequency deviations are small, the output of the auxiliaries changes a little. The effects of frequency deviations on the output of the auxiliaries are ignored in the conventional frequency response model. When a large frequency deviation occurs, the induction motor speed changes a lot. It makes the output of the auxiliaries decrease severely. The output of the auxiliaries affects the output power of the thermal power unit and constitutes a vicious circle. Therefore, it is necessary to consider the effects of frequency deviations on the auxiliary output in the frequency response model.

B. THE STRUCTURE OF THE EXTENDED FREQUENCY RESPONSE MODEL

The conventional single machine frequency response model simulates frequency dynamic behaviors of the power system with small disturbance. It considers the speed-governor, the steam turbine, the generator inertia swing equation, and some nonlinear constraints. The output power of the generator is proportional to the valve opening of the steam turbine with the assumption of constant boiler steam pressure. The conventional model is not suitable to analyze frequency dynamic behaviors and stability in an extensive frequency variation range. Therefore, more control modules affecting frequency dynamic behaviors and frequency deviation are necessary to be considered to solve this problem. The power system is a controlled system with many feedback loops, which considers the long-term effects of the control input. For the fossil-power plant, the auxiliaries are an essential part of the feedback loop in the whole control circuit for the thermal power unit. Some of the auxiliaries are equipped with a variable-frequency motor. The output of these auxiliaries is insensitive to frequency change. Therefore, an extended frequency response model is constructed in Fig.2, considering the effects of frequency deviation on boiler auxiliaries.

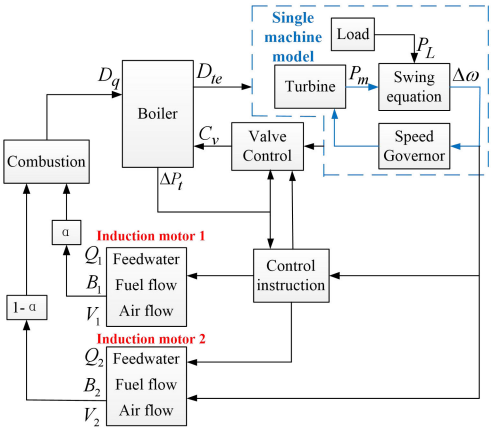

FIGURE 2. The structure of the extended frequency response model.

In Fig.2, P_m is the steam turbine mechanical power (p.u.). P_L is load (p.u.). $\Delta\omega$ is angular frequency deviation (p.u.), C_V presents the valve opening. ΔP_t is the boiler steam pressure deviation. Q_1, B_1, and V_1 are the feedwater flow, fuel flow, and airflow, respectively, of the output of the auxiliaries equipped with traditional induction motors. Q_2, B_2, and V_2 are the feedwater flow, fuel flow, and airflow, respectively, of the auxiliary output with the variable-frequency motors. α presents the percentage of the auxiliaries equipped with a variable-frequency motor. D_q is the heat released from furnace combustion (p.u.). D_{te} is the steam flow of the steam turbine(p.u.).

The typical component models in Fig.2 only consider the inertia link and do not consider energy losses. The influence of voltage change is little with active power deficits. The extended frequency response model has the following assumptions that need to be met. 1) The effects of frequency and voltage are coupled and mutual. This model only analyzes the impact of frequency deviations and ignores the influences of the voltage due to the time frame of interest in frequency dynamics is longer than the excitation system. 2) The steam flow and the feed water are balanced, and boiler steam flow evaporation is proportional to fuel flow. 3) The extended model does not consider frequency stability control measures and only considers the effects of frequency deviation on the output of boiler auxiliaries in the response process.

C. DETAILS OF THE EXTENDED FREQUENCY RESPONSE MODEL

The extended frequency response model is mainly based on a single machine model. The structure of the single machine

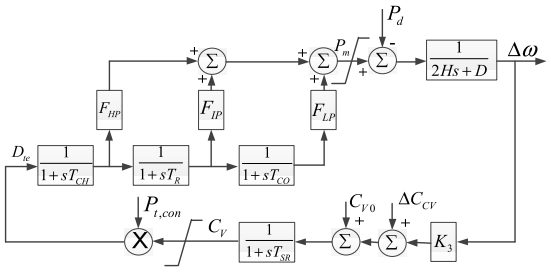

FIGURE 3. Single machine frequency response model.

model is shown in Fig.3. The variable value of model inputs and outputs is the nominal value unless otherwise stated. The steam turbine converts the kinetic energy of high-pressure steam into the rotor mechanical energy [26]. The input of the steam turbine is the steam flow, which is the product of the valve opening and boiler steam pressure. The output of the steam turbine is mechanical power [27]. The generator is reduced to the inertia swing equation considering the damping effect [12], [18]. The speed-governor module is a feedback control that uses frequency deviation and boiler pressure deviation signal to regulate the valve opening and boiler steam pressure [27].

In the single machine model, D is the damping coefficient. H is the generator inertia time constant (s). F_{HP}, F_{IP}, and F_{LP} are the high, intermediate, and low-pressure turbine power fraction, respectively, where $F_{HP} + F_{IP} + F_{LP} = 1$. T_{CH} is steam chest time constant (s). T_R is reheat time constant (s), T_{CO} is a crossover time constant (s), K_3 is the proportionality coefficient. T_{SR} is the speed relay time constant (s). $P_{t,con}$ is constant boiler steam pressure (=1.0 p.u.). ΔC_{CV} presents the instruction of the valve opening control from ΔP_t. C_{V0} is the initial valve opening.

In this paper, IEEE boiler dynamic nonlinear model is adopted [27], [28]. The boiler model is linked to the steam turbine model via the interface variable of boiler steam pressure. Boiler converts fossil fuel into thermal energy. Then the thermal energy is used to heat feedwater into high-pressure steam. The inputs of the boiler are the valve opening of the steam turbine and the heat release from furnace combustion. The output of the boiler is steam flow. The state equations of the boiler model are expressed as equation (2) and (3) [27].

$$D_{te} = k_6 P_t C_V \tag{1}$$

$$\dot{P}_t = k_2 k_3 \sqrt{P_b - P_t} - k_3 k_5 P_t C_V \tag{2}$$

$$\dot{P}_b = -k_1 k_2 \sqrt{P_b - P_t} + k_1 k_4 D_q \tag{3}$$

where P_t is boiler steam pressure (MPa). P_b is the boiler drum pressure (MPa). k_1 and k_2 are the heat storage coefficient of the boiler drum and steam pipe, respectively. k_3 is the equivalence heat storage time constant (s). k_4, k_5, and k_6 are the internal parameter to simulate mass and energy balance.

Speed-governor senses the frequency change to regulate the valve opening. The valve control module limits the valve opening of the steam turbine. The input of the valve control module includes the regulation instructions of the speed-governor module and the control system. The control instruction module simulates the coordination control system commands. The output of the valve control module is the valve opening. The state equations are expressed as equations (4) to (6) [27].

$$C_V = x_4 \tag{4}$$

$$\dot{x}_4 = (\Delta\omega K_3 + C_{V0} + \Delta C_{CV} - x_4) \cdot \frac{1}{T_{SR}} \tag{5}$$

$$\Delta C_{CV} = f(\Delta P_t) = K_5 \Delta P_t \tag{6}$$

where x_4 is the state variable of the speed-governor, K_5 is the proportionality coefficient.

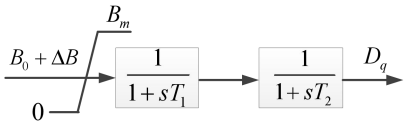

FIGURE 4. The coal mill and water-wall dynamic module.

Fuel is the primary energy source to produce heat by boiler furnace combustion. The dynamic process of boiler combustion is simplified with the inertia blocks of the coal mill and water-wall, which is shown as Fig.4 [27]. When a large frequency deviation occurs, the output of the fuel reaches the maximum value at a particular frequency.

In the coal mill and water-wall dynamic module, T_1 and T_2 are the inertial time constants. B_0 is the initial fuel in p.u. B_m is the maximum value of the output fuel flow of auxiliaries in p.u. ΔB is fuel regulation commands are related to $\Delta\omega$ and the output of the PI controller of steam pressure deviation.

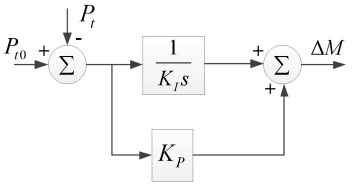

FIGURE 5. The steam pressure controller module.

The structure of the steam pressure controller of the boiler increases the fuel input to the boiler furnace, which is shown in Fig.5. In this module, K_P is the proportionality coefficient. K_I is the integral coefficient. P_{t0} is the rated value of the boiler steam pressure in MPa. ΔM is the change of the fuel flow (p.u.).

The auxiliaries sense the frequency change and then regulate feedwater and fuel to maintain boiler steam pressure stable. In fossil-power plant operation, it assumes that the temperature of the input water is invariable. The heat absorbed for converting water to steam is proportional to the input feedwater flow. The heat absorbed comes from fuel combustion. If the calorific value of the fuel remains unchanged, the change of the fuel should be proportional to the feedwater. According to actual operation data in one day,

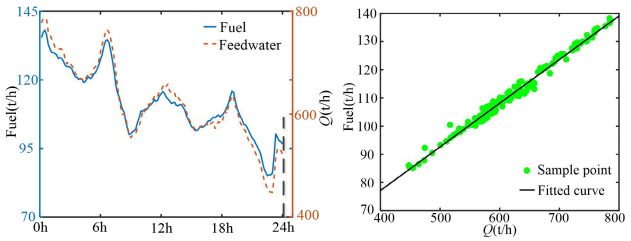

FIGURE 6. Relationship between feedwater and fuel. *(a)* the actual operation data; *(b)* the fitted curve of sample data.

the relationship between the fuel flow and feedwater flow is shown in Fig.6. The figure shows the fuel flow and the feedwater flow have the same change trend. The relationship between fuel flow and the feedwater flow is fitted as equation (7).

$$B = a \cdot Q + b \tag{7}$$

where a and b is the function coefficient obtained by analyzing actual operation data, Q is feedwater flow (t/h).

The input of the boiler is the heat release from boiler combustion, which is the output of the coal mill and water-wall module. The input of this module is the fuel flow. Therefore, the fuel flow is calculated based on feedwater flow with equation (7). The feedwater flow is the intermediate constraint variable in the extended frequency response model.

D. POWER-FREQUENCY CHARACTERISTICS OF THE FEEDWATER PUMP

The operation of the feedwater pumps plays an essential role in fossil-power plant operation. The power consumption percentage of the feedwater pumps in power plants is relatively large compared with other auxiliaries. This paper mainly takes the feedwater pump as an example for detailed analysis. The relationship between the feedwater and system angular frequency is shown as equation (8).

$$Q = \sqrt{(K_1\omega^2 - H_{st})/R} \tag{8}$$

where ω is system angular frequency in rad/s and $\omega = 2\pi f$, K_1 is the coefficient determined by the structure and the size of the feedwater pump. H_{st} is the resistance coefficient of static head, and R is the resistance of the water pipe.

Equation (8) is transformed into equation (9) and (10) with the definition of critical angular frequency ω_{st}.

$$\omega_{st} = \sqrt{\frac{H_{st}}{K_1}} \tag{9}$$

$$Q^2 = 4\frac{K_1}{R}\pi^2(f^2 - f_{st}^2) \tag{10}$$

where f is system frequency, f_{st} is the critical frequency.

The valve opening of the feedwater pump changes the value of variable R, so the R is a variable parameter. It makes the valve of the feedwater pump have different operating conditions and different feedwater flow at the rated frequency. In reference [29], it means that the tolerance frequency of the auxiliaries is about 46.5∼47.5Hz for the rated system frequency 50Hz. In other words, the allowable frequency deviation is about 5%∼7% of the rated value. Therefore, it assumes that the critical frequency of the feedwater pump is 95% of the rated frequency. According to the actual operation data, the feedwater flow and the critical frequency f_{st} are known quantities in equation (10). When the output of the generator is the maximum value, the output of feedwater pumps also is. Therefore, the maximum ratio value of K_1/R is calculated. The characteristic curve of the feedwater pump is shown in Fig.7.

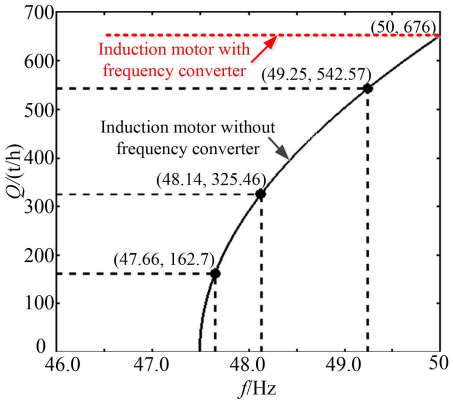

FIGURE 7. Power-frequency characteristic of the feedwater pump.

E. EXAMPLE OF THE EXTENDED FREQUENCY RESPONSE MODEL

The extended single machine frequency response model reflects the frequency dynamic behaviors in the long-term period. With load increasing disturbance of 0.185 p.u., the impact of the boiler and auxiliaries output on dynamic frequency behavior is demonstrated by MATLAB simulation. Tab.1 gives out the parameter values of the extended model. The comparison of the frequency response of the extended and conventional single machine models is shown in Fig.8.

TABLE 1. Typical parameter values of the extended single machine frequency response model.

Parameter	Value	Parameter	Value	Parameter	Value
k_1	0.0111	H	4	T_{SR}	0.1
k_2	3.5	F_{HP}	0.328	T_1	5
k_3	0.2	T_{CH}	0.297	T_2	30
k_4	4.167	F_{IP}	0.266	K_I	1/2200
k_5	0.2381	T_R	12.213	K_1/R	26.837
k_6	0.0571	F_{LP}	0.406	a	0.1549
D	1	T_{CO}	0.0974	b	15.195
P_{t0}	17.5	K_3	25	K_P	0.08

The conventional single machine model assumes that the boiler steam pressure as a constant, and the output power is only related to the valve opening of the steam turbine. In the frequency response process, the maximum frequency

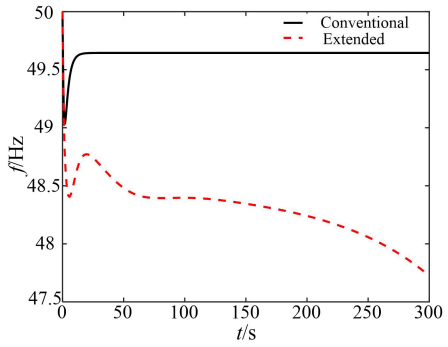

FIGURE 8. Frequency response curves comparison of the extended and conventional single machine model.

deviation is 0.95Hz. In the extended model, the boiler steam pressure is no longer maintaining a constant with the valve opening change. The output power of the steam turbine and the maximum frequency deviation are affected by the boiler steam pressure and the valve opening. The maximum frequency deviation of the extended model is 1.6Hz. In Fig.8, the difference between the maximum frequency deviations of the two models is 0.65Hz. Large frequency deviations make the output of the auxiliaries decrease. In this case, the boiler steam pressure and system frequency continue to decline in the long-term period. In the dynamic response process, the frequency of the extended model decrease to 47.75Hz at t = 300s. If the frequency stability control measures, such as UFLS, are not considered in the dynamic process, the system frequency is unstable.

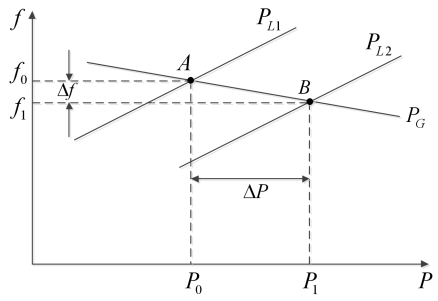

FIGURE 9. Conventional static power-frequency characteristic of the generating unit.

III. STATIC POWER-FREQUENCY CHARACTERISTICS

A. STATIC POWER-FREQUENCY CHARACTERISTIC WITHIN THE SMALL FREQUENCY VARIATION RANGE

The conventional static power-frequency characteristics of the thermal power unit in Fig.9 are usually illustrated as the straight line approximately with small frequency deviation variation. In Fig.9, P_G is the static power-frequency characteristic curve of generating unit. This curve defines the ability of the system to compensate for power imbalance at the cost of frequency deviation. When the generator operates at point A, the frequency is f_0, and the output power is P_0. If the load characteristic curve moves to P_{L2}, the speed-governor uses the frequency deviation signal to regulate the valve opening with the constant boiler steam pressure. The increasing output power of the generator is inversely proportional to frequency change. Finally, the frequency decreases to f_1, and the output power of the generator increases to P_1. The new equilibrium point is point B. The frequency deviation is Δf, and the change of the output power of the generator is ΔP.

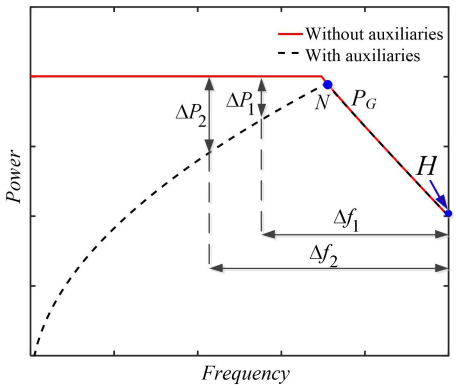

FIGURE 10. Static power-frequency characteristic of the thermal power unit considering auxiliaries frequency characteristic.

B. STATIC POWER-FREQUENCY CHARACTERISTIC WITHIN THE EXTENSIVE FREQUENCY VARIATION RANGE

The single machine system with the extended model is used to analyze the static power-frequency characteristic of the thermal power unit within the extensive frequency variation range in MATLAB Simulink environment. The auxiliaries are equipped with traditional induction motors in the extended model. In Fig.10, the point H firstly chosen as the initial steady-state operation point of the extended frequency response model at (f_N, P_0). Then, increasing a fixed small load disturbance of 0.002 p.u. is set to obtain the steady-state operation. According to the generator output power and frequency deviation in steady-state after disturbance, the generator regulation coefficient is calculated. And then, using the regulation coefficient of the generator and fixed frequency deviation df = 0.01Hz calculate generator output power. The results are recorded and are used as the initial steady-state operating point for the next simulation. Using MATLAB program control simulation and record the result. If the frequency characteristic of the auxiliaries is not considered, the output of the generator is going to reach the maximum value when the frequency decreases to a particular value. The static power-frequency characteristic curve of the thermal power unit is obtained within the extensive frequency variation range by repeating the steps above. When the valve opening reaches the maximum value, the output power of the generating unit reaches the maximum value [30]. This operating condition is the full-load operation. The output power of the generator maintains the maximum value with frequency dropping. The static power-frequency characteristic curve

of the generating unit without considering the auxiliaries is shown as the solid line in Fig.10.

However, if the frequency characteristic of the auxiliaries is considered, the performance of boiler feedwater pumps is affected by large frequency deviations. It reduces the output power of the generating unit [30]. In Fig.10, the static operating point moves to the constraint curve gradually. When the static operation points are on this constraint curve, the auxiliary output determines the output power of the generator. The power-frequency characteristic curve of the feedwater pumps is the output constraint curve of the generators. The static power-frequency characteristic curve of the generating unit produces an inflection point N. The output power of the generating unit is no longer monotonically increasing within the extensive frequency variation range. To the left part of the inflection point N on this curve, the steady-state operating points of the generating unit are obtained by the initialization of the frequency deviation, the steam flow, and the fuel flow. The static power-frequency characteristic curve of the generator is coincident with that of the auxiliaries. The static power-frequency characteristic curve of the generating unit within an extensive frequency variation range is shown as the dashed line in Fig.10 when considering the frequency characteristics of the auxiliaries.

According to the constraint of the feedwater flow, the value of the left part of the inflection point N is $2a * Q_m+b$. With equation (10) and the maximum ratio value of K_1/R, the maximum feedwater flow Q_m is calculated. In Fig.10, the effect the frequency deviations on the output of the auxiliaries is described as $1\text{-}2a * Q_m+b$. Therefore, the ΔP_1 and ΔP_2 are calculated quantitatively, respectively, with frequency deviation Δf_1 and Δf_2. In Fig.10, if the initial steady-state operating condition is (50Hz, 0.6 p.u.), the $\Delta f_1 = 1.375$Hz, $\Delta f_2 = 2.025$Hz, and the $\Delta P_1 = 0.2$p.u., $\Delta P_2 = 0.45$p.u. The larger the frequency deviations are, the more severe effects on the output power are.

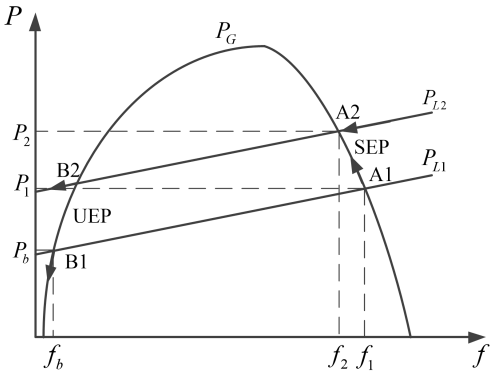

FIGURE 11. The static power-frequency characteristic analysis.

C. STATIC STABILITY ANALYSIS OF EQUILIBRIUM POINTS

The static power-frequency characteristic curve of the generating unit has the curled-back characteristic, so it produces two equilibrium points with a given load characteristic shown as Fig.11. In Fig.11, P_G is the static power-frequency characteristic curve of the generating unit. For the load frequency characteristic P_{L1}, the equilibrium points are A1 and B1. For P_{L2}, the equilibrium points are A2 and B2. No matter which load characteristic is, both of the equilibrium points can satisfy the balance between generation and load. However, the stability characteristics of these two static equilibrium points are different after being subjected to disturbance.

For point A1, the frequency is f_1, and the load is P_1. If a disturbance makes the load characteristic P_{L1} move to P_{L2}, the generating unit reduces unbalanced power with the cost of frequency deviation. The output power of the generating unit increases and the power balance is reestablished at point A2. Therefore, the system can restore to an equilibrium state for any small disturbance within the vicinity of the point A1. The equilibrium point A1 is called the frequency stable equilibrium point (SEP). For point B1, the frequency is f_b, and the load is P_b. If frequency decreases a little, the output power of the generating unit decrease, and then the frequency continues to drop. The system moves away from the equilibrium point due to the load is greater than the generation. The system is unable to restore to an equilibrium state and even frequency collapse. Therefore, the equilibrium point B1 is called frequency unstable equilibrium point (UEP).

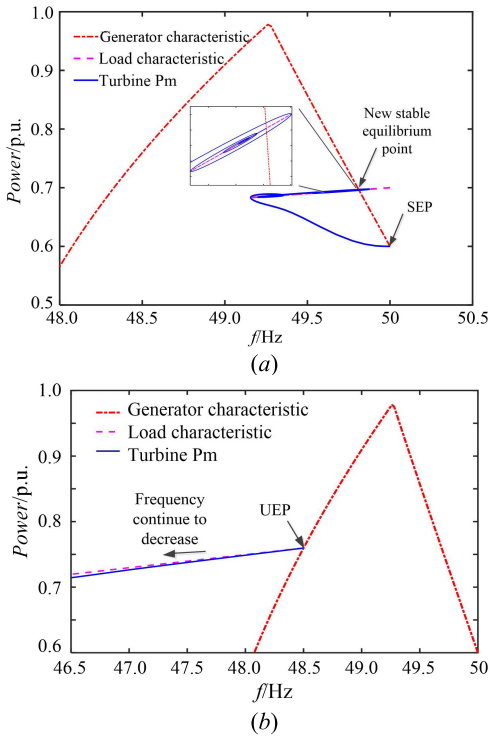

FIGURE 12. Frequency stability characteristic analysis. *(a)* the scenario at point A1 in Fig.11; *(b)* the scenario at point B1 in Fig.11.

The single machine system with the extended model MATLAB simulation shows that the stability characteristics with disturbance of these two equilibrium points in Fig.12. The model parameters are shown in Tab.1. Fig.12(a) simulates the

stability characteristic of SEP. The initial frequency deviation is 0 p.u. and the mechanical power, steam flow, and fuel flow are 0.6 p.u. Boiler steam pressure is rated value. According to the initial setting, the initial steady-state operating point is (50Hz, 0.6 p.u.), and disturbance is 0.1 p.u. After the disturbance, system frequency restores stable. Fig.12(b) simulates the stability characteristic of UEP. In steady-state operating conditions, the mechanical power is determined by $P_m = P_L + D\Delta f_*$. The initial frequency deviation is set as -0.03 p.u. The initial mechanical energy value, the steam flow value, and the fuel flow value are 0.7596 p.u. The initial load is 0.7896 p.u. According to the initial setting and simulation, the initial steady-state operating point is (48.5Hz, 0.7596 p.u.) on the left part of the generator power-frequency characteristic. The effects of frequency deviations (1.5Hz) on the output power are 0.2404 p.u. The disturbance is 1e-4 p.u. In system actual operation, the steady-state operating point is not able to be on the UEP, but it exists in theory analysis. After the disturbance, system frequency is unstable. The dynamic simulation results are consistent with the analysis above.

The nonlinear state equations of the extended frequency response model are linearized to discuss the stability characteristics near the equilibrium points. Then the eigenvalues of the coefficient matrix of the state equations are calculated to identify system stability. If all the eigenvalues of the coefficient matrix have negative real parts, the original nonlinear system is stable near the equilibrium point. Otherwise, the original nonlinear system is unstable.

When the system operates at SEP, the actual auxiliary output is smaller than the maximum output. The basic parameters of the extended frequency response model are given in Tab.1. The system eigenvalues are shown in Fig.13. From the Fig.13, all eigenvalues have negative real parts, so the original nonlinear system is stable near the equilibrium point.

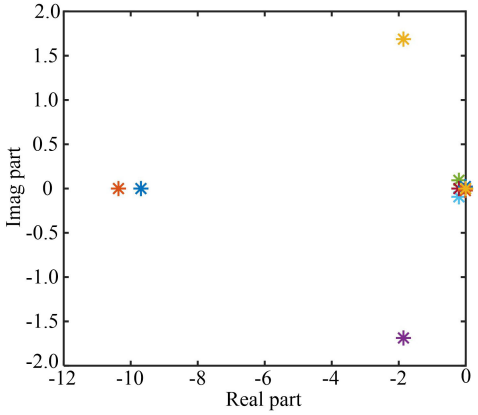

FIGURE 13. The eigenvalues of the system when initial operation condition at SEP.

When the system operates at UEP, the output of the auxiliaries is the maximum value. Therefore, the maximum value of the fuel output is B_m, which changes the state equations of the boiler combustion module. The basic parameters of

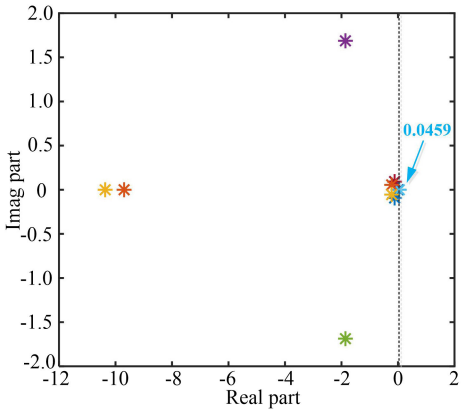

FIGURE 14. The eigenvalues of the system when initial operation condition at UEP.

the extended frequency response model are given in Tab.1. The system eigenvalues of the extended model are shown in Fig.14. Because there is an eigenvalue with a positive real part, the nonlinear system is unstable at UEP. The eigenvalue with the positive real part is marked in Fig.14.

IV. QUANTITATIVE FREQUENCY STABILITY ASSESSMENT

A. DIFFERENCE BETWEEN FREQUENCY SECURITY AND FREQUENCY STABILITY ASSESSMENT

Frequency security refers to the ability of a power system to transit to a new operating condition without violating physical constraints. The requirements for transient frequency deviation security assessment are described by a two-element table $[f_{\text{th}}, t_{\text{th}}]$. In the table, f_{th} is the given frequency threshold. t_{th} is the duration of abnormal frequency less than f_{th}. It is the basis for frequency security assessment in the transient process. If the duration of frequency deviating from f_{th} exceeds t_{th}, the system transient frequency deviation is insecure.

Power system frequency stability refers to the ability of a power system to maintain steady frequency following a severe system upset, resulting in a significant imbalance between generation and load [8]. However, most existing frequency stability assessment researches consider the acceptability of steady-state frequency deviation. It mainly depends on frequency response trajectory, and then frequency stability is judged by whether or not the system frequency restores to an acceptable range. Frequency stability assessment is confused with the frequency security assessment. The main difference between frequency stability and frequency security assessment is that frequency security analyzes the relationship between frequency response trajectory and the given requirement. Frequency stability is the characteristic of the interaction between the frequency and power change of the system itself.

The power system is a constrained dynamic system, as their state trajectories are restricted to a particular subset in state-space denoted as the feasible operating region [8]. If a disturbance makes operation trajectory exit the desired region,

it leads to system structure change or unstable operation. The desired region is the restricted disturbance region.

B. QUANTITATIVE STATIC FREQUENCY STABILITY INDEX

For assessing the degree of static frequency stability, it is necessary to calculate the frequency value of SEP and UEP. According to the state equations of the steam turbine, the boiler, the coal mill, water-wall, and the auxiliary modules in steady-state, the expression of the left side of generator static power-frequency characteristic is shown as equation (11). The load frequency characteristic curve is shown as equation (12).

$$P_m = \frac{k_4 k_6}{k_5}(2aQ + b) \tag{11}$$

$$P_L = P_0 + \Delta P + D\Delta f_* \tag{12}$$

where P_0 is the initial load, ΔP is load disturbances. Δf_* is the nominal value of frequency deviation.

Then the expression of UEP frequency is derived as equation (13) from equation (11) and (12).

$$(C_3 - 9D^2)f^2 - 6C_1Df - (C_1^2 + C_2C_3) = 0 \tag{13}$$

where $C_1 = (P_0 + \Delta P - 1) - b$, $C_2 = f_{st}^2$, $C_3 = 16 \cdot \pi^2 \cdot a^2 \cdot K_1/R$.

The UEP frequency is associated with some factors, such as the initial load, the power-frequency characteristics of the auxiliaries, load disturbance, the damping coefficient, and the relationship between feed water and fuel. The solutions are obtained by using the solution formula of a quadratic function (13). One of the solutions is dropped due to its irrationality.

The expression of the right side of the static power-frequency characteristic of the generating unit is regarded as a linear equation approximately as follows.

$$P_m = P_0 + K_G\Delta f_* \tag{14}$$

where K_G is the frequency regulation coefficient.

By a single machine system, the initial steady-state operation condition is (50Hz, 0.6 p.u.) The whole load frequency characteristic is $P_L = P_0 + D\Delta\omega$. According to the method in section III, the static frequency characteristic curves of the generating unit and different loads are obtained and shown in Fig.15. The system operating at load characteristic 1 can withstand the larger disturbance. The load characteristic 1 has a better stability degree compared with other load characteristics.

A quantitative index for frequency static stability assessment is proposed to evaluate the difference of frequency stability between different load characteristics, which is equation (15).

$$\eta = \frac{f_{SEP} - f_{UEP}}{f_N} \tag{15}$$

where η is the assessment index ($0 \le \eta \le 0.05$). f_{SEP} and f_{UEP} present the frequency value of SEP and UEP, respectively. The minimum value of f_{UEP} is 95% of the rated frequency value, and f_N is the rated frequency value.

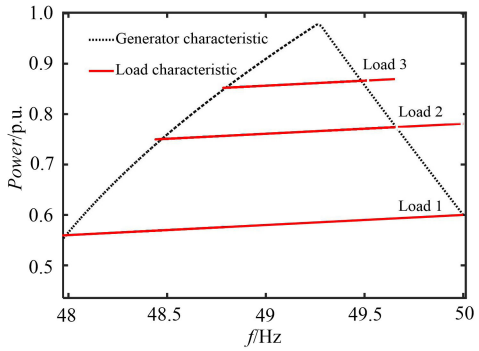

FIGURE 15. Static power-frequency characteristic curves of generator and loads.

V. CASE STUDY

A. STABLE SCENARIOS

According to the analysis above, if the system operates at the SEP, the system frequency is stable but maybe insecure [31]. A provincial power grid in China is used to simulate the frequency dynamic process and to analyze frequency characteristics with PSS/E. The total installed capacity of the system is 69 008MW. The total load is 58 876MW. The initial disturbance is generator tripping and the active power loss 7 000MW. When the frequency increases to 49.23Hz in the first recovery procedure, some renewable energy generating units are cut off to simulate the distributed renewable energy secondary exiting operation. The active power loss is 2 480MW. In the dynamic response processes, there are two scenarios. Scenario 1 considers the UFLS control measure, but scenario 2 does not. The frequency response curves of different scenarios are shown in Fig.16. In scenario 1, the system frequency is restored to a stable but insecure range. In scenario 2, system frequency is restored to a stable and secure range. In this example, scenario 2 with UFLS control has better stability characteristics compared with scenario 1.

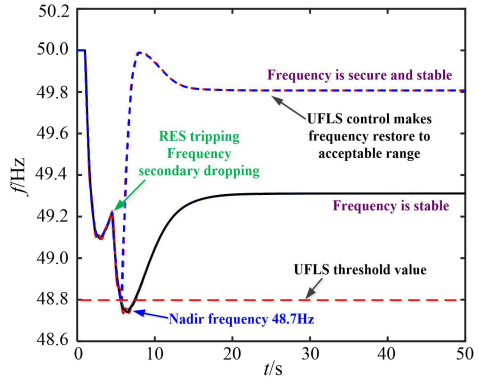

FIGURE 16. The frequency response of the system after disturbance.

Using the proposed quantitative index for static frequency stability assessment in section IV compares the degree of static frequency stability with different load characteristics by

TABLE 2. Static frequency stability quantitative assessment.

Load characteristic	f_{SEP}(Hz)	f_{UEP}(Hz)	η	ΔP_{max}(p.u.)
Load 1	50.00	47.9876	0.0402	0.18106
Load 2	49.6569	48.4727	0.0237	0.09536
Load 3	49.4835	48.7975	0.0137	0.05193

using a single machine model in MATLAB. The quantitative index reflects the system static frequency stability differences among different load characteristics. The greater this index is, the better the static stability characteristics system has. The stability degrees of the load characteristics 1, 2, and 3 in Fig.15 are compared. Tab.2 shows the quantitative assessment index and the maximum disturbance that the system can withstand. The maximum disturbance (ΔP_{max}) is obtained by continuously increasing load disturbance until system frequency unstable.

With the load characteristic curve changing from load 1 to load 3, the quantitative assessment index of frequency stability decreases. Then the static frequency stability of different initial P_0 under the rated frequency is also analyzed. The results are shown in Tab.3. If the smaller the initial load is, the system can withstand more severe disturbance, and the larger the index and the better stability is.

TABLE 3. Frequency stability assessment with different initial P_0.

P_0(p.u.)	f_{SEP}(Hz)	f_{UEP}(Hz)	η	ΔP_{max}(p.u.)
0.6	50.0	47.9876	0.0402	0.18106
0.7	50.0	48.2344	0.0353	0.14828
0.8	50.0	48.5334	0.0293	0.11539

If the given disturbance is smaller than ΔP_{max}, the system is stable. Hence, large-disturbance stability always refers to a specified disturbance scenario. A stable equilibrium set has a finite disturbance region of attraction. The larger the disturbance region, the better the stability the system has.

B. UNSTABLE SCENARIOS

The extended single machine model is used to analyze the frequency dynamic behaviors in a single machine system with MATLAB to illustrate the unstable scenarios. The initial load is 0.6 p.u. When the load increases, the imbalance is initially covered by the generator rotor kinetic energy and makes the rotor speed decrease. The speed-governor changes the valve opening to release stored energy in the boiler. Then the main steam flow and the mechanical power of the steam turbine are increased.

When the load disturbance is larger than ΔP_{max}, large active power deficits lead to a significant frequency deviation. Large frequency deviations decrease the output of the auxiliaries and then further affect the output of the boiler. Generator and boiler regulation ability are unable to sustain for a long time when boiler steam pressure decreases with the valve opening increasing. If the output of boiler auxiliaries reduces significantly, the deterioration in the performance of boiler output does not be restrained. The boiler steam pressure continues to decline, which makes the regulation ability of the boiler weak, and generator output power continues to decline. When the valve opening reaches the maximum value, boiler steam pressure further decreases. Finally, the active power deficit is further increased, which leads to continuously decreasing in frequency and, eventually, frequency collapse. In the single machine system with the extended model, the disturbance is load increasing by 0.185 p.u. Fig.17 shows the dynamic response process of boiler steam pressure when the system frequency is unstable.

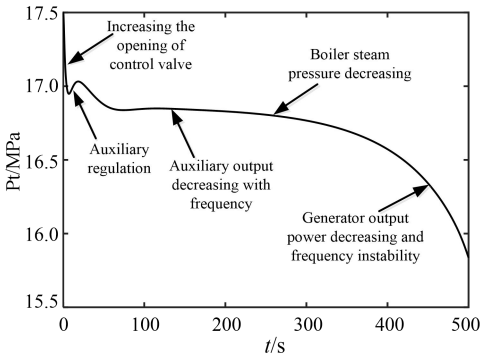

FIGURE 17. Dynamics of boiler main steam pressure.

In the IEEE 39-bus system, the total installed capacity of the system generators is 6800MW, and the total load is 6140.8MW. The dynamic models all use the typical model and typical parameter values. The system disturbance is 1080MW, which is generator tripping at bus 30 and 38. The disturbance amount is 15.88% of the installed capacity of the whole system. The frequency response curves with PSS/E simulation are shown in Fig.18 with different scenarios and different model extensions.

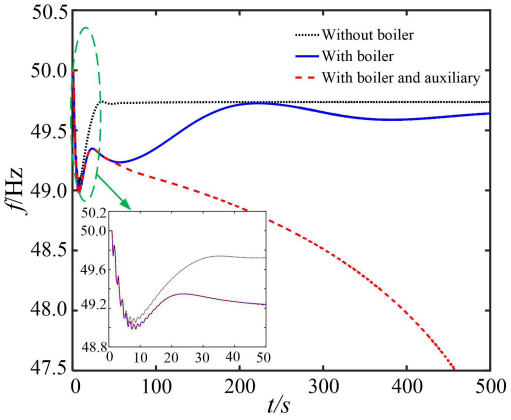

FIGURE 18. Frequency response with large disturbance.

The example shows that the recovery process of the system frequency is longer due to dynamic boiler response. When the auxiliaries are further considered, large frequency deviations

affect the output of auxiliaries. Then, it affects boiler steam pressure, steam flow, and the output mechanical power of the steam turbine. Eventually, the system frequency continues to decrease and until frequency instability or collapse.

From the analysis above, it reveals that the main reasons for frequency continuously dropping are the active power balance is unable to be maintained and the weakening of boiler regulation ability. When large frequency deviations are experienced, the output of the auxiliaries decreases severely. It affects the boiler operation condition and results in continuously reducing the boiler steam pressure. The boiler steam pressure that is affected by auxiliary output is unable to restore to the standard value. This situation accelerates the frequency deterioration process, which results in unplanned generator tripping and cascading faults.

C. SCENARIOS WITH VARIABLE-FREQUENCY MOTOR

In the fossil-power plant, the output of the auxiliaries equipped with the variable-frequency motors is insensitive to frequency change. The single machine system is used to analyze the effects of the output of the auxiliaries equipped with the variable-frequency motor on frequency dynamic behaviors with MATLAB. The parameters are shown in Tab.1. The disturbance is load increasing by 0.2 p.u. In scenario 1, the auxiliaries are equipped with traditional induction motors. In scenario 2, there are 30% of the auxiliaries equipped with variable-frequency motors. The frequency responses of the two situations are shown in Fig.19. The auxiliaries equipped with the variable-frequency motor can maintain a stable output with a large frequency deviation. The output of the auxiliaries makes boiler steam pressure restore to the standard value. The mechanical power continues to increase to restore the balance between generation and load.

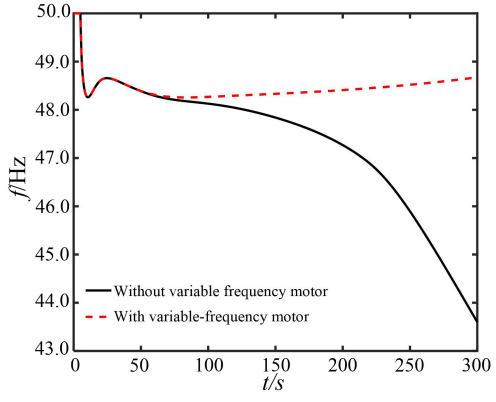

FIGURE 19. Frequency response considering auxiliaries equipped with a variable-frequency motor.

VI. CONCLUSIONS

An extended frequency response model for long-term frequency stability assessment is constructed, considering the frequency characteristics of the auxiliaries. The static power-frequency characteristic of the thermal power unit is no longer monotonically increasing with system frequency dropping when considering the frequency characteristic of the auxiliaries in the extended model. There is an inflection point on the static power-frequency characteristic curve of the thermal power unit. The output power of the generator decreases rapidly with frequency declination to the left part of the inflection point on this curve. The static power-frequency characteristic curves of the thermal power unit and the load have two equilibrium points. These two equilibrium points have different stability characteristics, and one of the points with a significant frequency deviation is the frequency UEP. Based on UEP, the proposed frequency stability quantitative index can describe and compare the degree and the difference of static frequency stability quantitatively. The performance of the auxiliaries equipped with the variable-frequency motors restrain the frequency deterioration process effectively and improve the frequency stability characteristics.

In this paper, only the systems with dominant thermal power generating units are studied with frequency reduction cases. Moreover, this paper mainly discusses static frequency stability assessment. Therefore, system frequency characteristics analysis with other types of generators, over frequency cases, and the dynamic frequency stability quantitative assessment need be further discussed in the following study.

REFERENCES

[1] H. Gu, R. Yan, and T. K. Saha, "Minimum synchronous inertia requirement of renewable power systems," *IEEE Trans. Power Syst.*, vol. 33, no. 2, pp. 1533–1543, Mar. 2018.

[2] Q. Wu, Y. Huang, C. Li, Y. Gu, H. Zhao, and Y. Zhan, "Small signal stability of synchronous motor-generator pair for power system with high penetration of renewable energy," *IEEE Access*, vol. 7, pp. 166964–166974, 2019.

[3] Z. Chen, "Wind power in modern power systems," *J. Modern Power Syst. Clean Energy*, vol. 1, no. 1, pp. 2–13, Jun. 2013.

[4] National Grid ESO. *Interim Report into the Low Frequency Demand Disconnection (LFDD) Following Generator Trips and Frequency Excursion on 9 Aug 2019*. Accessed: Feb. 27, 2020. [Online]. Available: https://www.ofgem.gov.uk/system/files/docs/2019/08/incident_report_lfdd_-_summary_-_final.pdf

[5] Australian Energy Market Operator. (Oct. 2016). *Update Report—Black system event in South Australia on 28 September 2016*. Accessed: Feb. 27, 2020. [Online]. Available: https://www.aemo.com.au/-/media/Files/Media_Centre/2016/AEMO_19-October-2016_SA-UPDATE-REPORT.pdf

[6] Z. A. Obaid, L. M. Cipcigan, L. Abrahim, and M. T. Muhssin, "Frequency control of future power systems: Reviewing and evaluating challenges and new control methods," *J. Mod. Power Syst. Clean Energy*, vol. 7, no. 1, pp. 9–25, 2019.

[7] Y.-Q. Bao, Y. Li, B. Wang, M. Hu, and P. Chen, "Demand response for frequency control of multi-area power system," *J. Modern Power Syst. Clean Energy*, vol. 5, no. 1, pp. 20–29, Jan. 2017.

[8] P. Kundur, J. Paserba, V. Ajjarapu, G. Andersson, A. Bose, C. Canizares, N. Hatziargyriou, D. Hill, A. Stankovic, C. Taylor, T. Van Cutsem, and V. Vittal, "Definition and classification of power system stability IEEE/CIGRE joint task force on stability terms and definitions," *IEEE Trans. Power Syst.*, vol. 19, no. 3, pp. 1387–1401, Aug. 2004.

[9] *Final Report of the Investigation Committee on the 28 September 2003 Blackout in Italy*, UCTE, Brussels, Belgium, 2004.

[10] G. Andersson, P. Donalek, R. Farmer, N. Hatziargyriou, I. Kamwa, P. Kundur, N. Martins, J. Paserba, P. Pourbeik, J. Sanchez-Gasca, R. Schulz, A. Stankovic, C. Taylor, and V. Vittal, "Causes of the 2003 major grid blackouts in north america and europe, and recommended means to improve system dynamic performance," *IEEE Trans. Power Syst.*, vol. 20, no. 4, pp. 1922–1928, Nov. 2005.

[11] R. Yan, N.-A.-Masood, T. Kumar Saha, F. Bai, and H. Gu, "The anatomy of the 2016 South Australia blackout: A catastrophic event in a high renewable network," *IEEE Trans. Power Syst.*, vol. 33, no. 5, pp. 5374–5388, Sep. 2018.

[12] P. He, B. Wen, and H. Wang, "Decentralized adaptive under frequency load shedding scheme based on load information," *IEEE Access*, vol. 7, pp. 52007–52014, 2019.

[13] H. Zhang, C. Li, and Y. Liu, "Quantitative frequency security assessment method considering cumulative effect and its applications in frequency control," *Int. J. Electr. Power Energy Syst.*, vol. 65, pp. 12–20, Feb. 2015.

[14] L. Zhao, X. Li, M. Ni, T. Li, and Y. Cheng, "Review and prospect of hidden failure: Protection system and security and stability control system," *J. Modern Power Syst. Clean Energy*, vol. 1, no. 1, pp. 1–9, Jun. 2015.

[15] *PSS/E Program Application Manual(V33.5)*, PTI Inc. Siemens Power Transmiss. & Distrib. Inc., Erlangen, Germany, 2013.

[16] M. Chan, R. Dunlop, and F. Schweppe, "Dynamic equivalents for average system frequency behavior following major distribances," *IEEE Trans. Power App. Syst.*, vol. PAS-91, no. 4, pp. 1637–1642, Jul. 1972.

[17] Q. Shi, F. Li, and H. Cui, "Analytical method to aggregate multi-machine SFR model with applications in power system dynamic studies," *IEEE Trans. Power Syst.*, vol. 33, no. 6, pp. 6355–6367, Nov. 2018.

[18] P. M. Anderson and M. Mirheydar, "A low-order system frequency response model," *IEEE Trans. Power Syst.*, vol. 5, no. 3, pp. 720–729, Aug. 1990.

[19] I. Roytelman and S. M. Shahidehpour, "A comprehensive long term dynamic simulation for power system recovery," *IEEE Trans. Power Syst.*, vol. 9, no. 3, pp. 1427–1433, Aug. 1994.

[20] Z. W. Li, X. Wu, K. Zhuang, L. Wang, Y. Miao, and B. Li, "Analysis and reflection on frequency characteristics of East China grid after bipolar locking of '9.19' Jinping-Sunan DC transmission line," *Autom. Electr. Power Syst.*, vol. 41, no. 7, pp. 149–155, 2017.

[21] M. E. Flynn and M. J. O'Malley, "A drum boiler model for long term power system dynamic simulation," *IEEE Trans. Power Syst.*, vol. 14, no. 1, pp. 209–217, Feb. 1999.

[22] J. O'Sullivan, M. Power, M. Flynn, and M. O'Malley, "Modeling of frequency control in an island system," in *Proc. IEEE Power Eng. Soc. Winter Meeting*, New York, NY, USA, Feb. 1999, pp. 574–579.

[23] G. Zhou, J. H. Lu, H. Q. Wei, X. H. Ma, and B. G. Cheng, "Study and application of optimal control strategy for automatic generator control (AGC)," *Electr. Power*, vol. 37, no. 1, pp. 57–61, Jan. 2004.

[24] P. Kundur, *Power System Stability and Control*. New York, NY, USA: McGraw-Hill, 1994.

[25] K. Liu and X. Wang, "Dynamic frequency simulation and study on turbine-generator including the effect of boiler and fuel system," in *Proc. Asia–Pacific Power Energy Eng. Conf.*, 2010, pp. 1–4.

[26] B. Vahidi, M. Tavakoli, and W. Gawlik, "Determining parameters of Turbine's model using heat balance data of steam power unit for educational purposes," *IEEE Trans. Power Syst.*, vol. 22, no. 4, pp. 1547–1553, Nov. 2007.

[27] Working Group on Prime Mover and Energy Supply Models for System Dynamic Performance Studies, "Dynamic models for fossil fueled steam unit in power system studies," *IEEE Trans. Power Syst.*, vol. 6, no. 2, pp. 753–761, May 1991.

[28] R. A. Naghizadeh, B. Vahidi, and M. R. Bank Tavakoli, "Estimating the parameters of dynamic model of drum type boilers using heat balance data as an educational procedure," *IEEE Trans. Power Syst.*, vol. 26, no. 2, pp. 775–782, May 2011.

[29] B. Cai, *Power System Frequency*. Beijing, China: China Electric Power Press, 1998.

[30] J. Machowski, Z. Lubosny, J. W. Bialek, and J. R. Bumby, *Power System Dynamics Stability and Control*. London, U.K.: Wiley, 2008.

[31] *GB 38755-2019 Code on Security and Stability for Power System*, State Admin. Market Regulation Standarization Admin. P. R. China, Beijing, China, Dec. 2019.

YUZHENG XIE received the B.E. and M.S. degrees from the Shandong University of Technology, Jinan, China, in 2014 and 2017, respectively. He is currently pursuing the Ph.D. degree with the Key Laboratory of Power System Intelligent Dispatch and Control of the Ministry of Education (Shandong University), China. His research interests include power system security and stability assessment, and power system control.

CHANGGANG LI (Member, IEEE) received the B.E. and Ph.D. degrees in electrical engineering from Shandong University, Jinan, China, in 2006 and 2012, respectively. He was a Research Scholar with the School of Electrical Engineering and Computer Science, The University of Tennessee, Knoxville, from 2012 to 2014. He is currently an Associate Research Fellow with the School of Electrical Engineering, Shandong University. His research interest is power system operation and control.

HENGXU ZHANG (Member, IEEE) received the B.E. degree from the Shandong University of Technology, in 1998, and the M.S. and Ph.D. degrees in electrical engineering from Shandong University, in 2000 and 2003, respectively. He is currently a Professor with the Key Laboratory of Power System Intelligent Dispatch and Control of the Ministry of Education (Shandong University), China. His main research interests include power system security and stability assessment, power system monitoring, and numerical simulation.

HUADONG SUN (Senior Member, IEEE) received the B.E. and M.S. degrees in electrical engineering from Shandong University, Jinan, China, in 1999 and 2001, respectively, and the Ph.D. degree from the China Electric Power Research Institute (CEPRI), Beijing, China, in 2005. He is currently the Vice President and also a Full Professor of electrical engineering with CEPRI. His research interests include power system analysis and power system operation and control.

VLADIMIR TERZIJA received the Dipl-Ing., M.Sc., and Ph.D. degrees in electrical engineering from the University of Belgrade, Belgrade, Serbia, in 1988, 1993, and 1997, respectively. He is the Engineering and Physical Science Research Council Chair Professor of power system engineering with the School of Electrical and Electronic Engineering, University of Manchester, Manchester, U.K., where he has been since 2006. From 1997 to 1999, he was an Assistant Professor with the University of Belgrade. From 2000 to 2006, he was a senior specialist for switchgear and distribution automation with ABB AG Inc., Ratingen, Germany. His current research interests include smart grid application of intelligent methods to power system monitoring, control, and protection; wide-area monitoring, protection, and control; switchgear and fast transient processes; and digital signal processing applications in power systems.